

Research paper

Unbiased roughness measurements: Subtracting out SEM effects

Gian F. Lorusso^a, Vito Rutigliani^a, Frieda Van Roey^a, Chris A. Mack^{b,*}^a Imec, IMEC, Kapeldreef 75, B-3001 Leuven, Belgium^b Fractilia, LLC, 1605 Watchhill Rd, Austin, TX 78703, USA

ARTICLE INFO

Article history:

Received 2 November 2017

Received in revised form 3 January 2018

Accepted 6 January 2018

Available online 6 January 2018

Keywords:

Line-edge roughness

Linewidth roughness

Stochastic-induced roughness

LER

LWR

Power spectral density

PSD

CD-SEM

ABSTRACT

Most scanning electron microscope (SEM) measurements of pattern roughness today produce biased results, combining the true feature roughness with noise from the SEM. Further, the bias caused by SEM noise changes with measurement conditions and with the features being measured. The goal of unbiased roughness measurement is to both provide a better estimate of the true feature roughness and to provide measurements that are independent of measurement conditions. Using an inverse linescan model for edge detection, the noise in SEM edge and width measurements can be measured and removed statistically from roughness measurements. This approach was tested using different pixel sizes, magnifications, and frames of averaging on several different post-lithography and post-etch patterns. Over a useful range of metrology conditions, the unbiased roughness measurements were effectively independent of these metrology parameters.

© 2018 Elsevier B.V. All rights reserved.

1. Introduction

Lithography and patterning advances continue to propel Moore's Law by cost-effectively shrinking the area of silicon consumed by a transistor in an integrated circuit. Besides the obvious need for improved resolution, these lithography advances must also allow good control of the smaller features being manufactured. Besides the normal "global" sources of variation that affect patterning fidelity (exposure dose and focus variations, hotplate temperature non-uniformity, scanner aberrations, etc.), small features also suffer from "local" variations caused by the fundamental stochastic randomness of patterning near the molecular scale. This stochastic-induced variation continues to be one of the major concerns for semiconductor patterning at the 10-nm node and below (with feature sizes below 40 nm). Stochastic effects can reduce the yield and performance of semiconductor devices in several ways:

- Within-feature roughness can affect the electrical properties of a device, such as metal line resistance and transistor gate leakage;
- Feature-to-feature size variation caused by stochastics (also called local CD uniformity, LCDU) adds to the total budget of CD variation, sometimes becoming the dominant source;
- Feature-to-feature pattern placement variation caused by stochastics (also called local pattern placement error, LPPE) adds to the total

budget of PPE, sometimes becoming the dominant source;

- Rare events leading to greater than expected occurrence of catastrophic bridges or breaks are more probable if error distributions have fat tails;
- Decisions based on metrology results (including process monitoring and control, as well as the calibration of OPC models) can be poor if those metrology results do not properly take into account stochastic variations.

For these reasons, proper measurement and characterization of stochastic-induced roughness is critical. Unfortunately, current roughness measurements (such as the measurement of linewidth roughness, LWR, or line-edge roughness, LER, using a critical dimension scanning electron microscope, CD-SEM) are contaminated by large amounts of measurement noise caused by the CD-SEM. This results in a biased measurement, where the true roughness adds in quadrature with the measurement noise to produce an apparent roughness that overestimates the true roughness. Furthermore, these biases are dependent on the specific CD-SEM tool used and on its settings. In this context, prior attempts at providing unbiased roughness estimates [1–6] often struggle in many of today's applications due to the smaller feature sizes and higher levels of SEM noise. As will be shown, these biases are also a function of the patterns being measured.

In this study, a new technique for producing unbiased estimates of roughness parameters will be investigated. It is based on the use of an analytical model for SEM scattering behavior that predicts linescans

* Corresponding author.

E-mail address: chris@lithoguru.com (C.A. Mack).

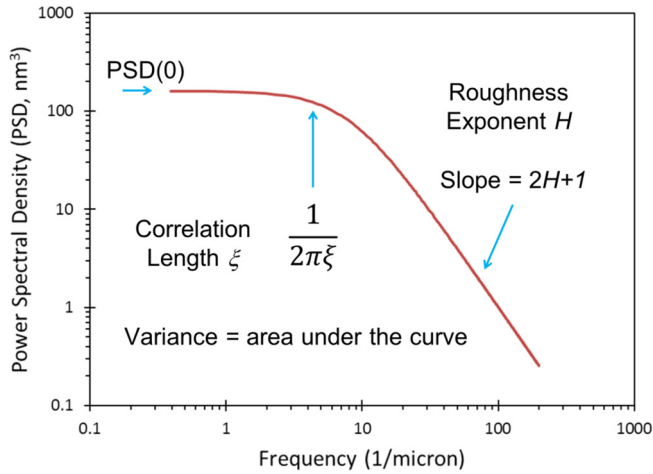


Fig. 1. A typical PSD can be described by three parameters: PSD(0), the low-frequency value of the PSD, the correlation length ξ , and the roughness exponent H . The variance of the roughness is the area under the PSD curve. Figure from Ref. 7.

for a given feature geometry. Run in reverse, an Inverse Linescan Model can be used for edge detection in such a way that SEM noise can be adequately measured and statistically subtracted from the roughness measurement, thus providing unbiased estimates of the roughness parameters. To test this technique, several sample datasets (each with set roughness characteristics) will be measured under a variety of CD-SEM conditions: SEM pixel size, magnification, and number of measurement frames averaged (i.e., electron dose). Ideally, each of these measurement tool settings will only have negligible impact on the unbiased roughness measurements, even though they are known to have a significant impact on biased roughness measurements.

2. Unbiased roughness measurement

Rough features are most commonly characterized by the standard deviation of the edge position (for LER), linewidth (for LWR), or feature centerline for pattern placement roughness (PPR). However, a frequency analysis of the roughness is required to fully describe the roughness, most commonly by using the power spectral density (PSD). The discussion in this section is based on the description of measuring unbiased power spectral densities of rough lines and spaces given in Reference 7.

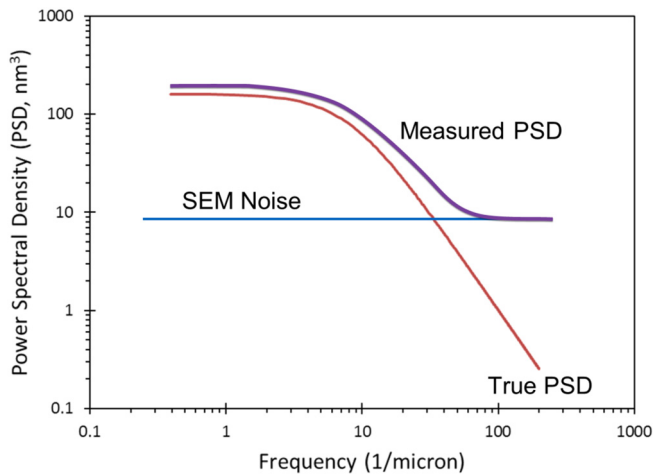


Fig. 2. The principle of noise subtraction: using the power spectral density, measure the flat noise floor in the high-frequency portion of the measured PSD, then subtract this white noise to get the true PSD. Figure from Ref. 7.

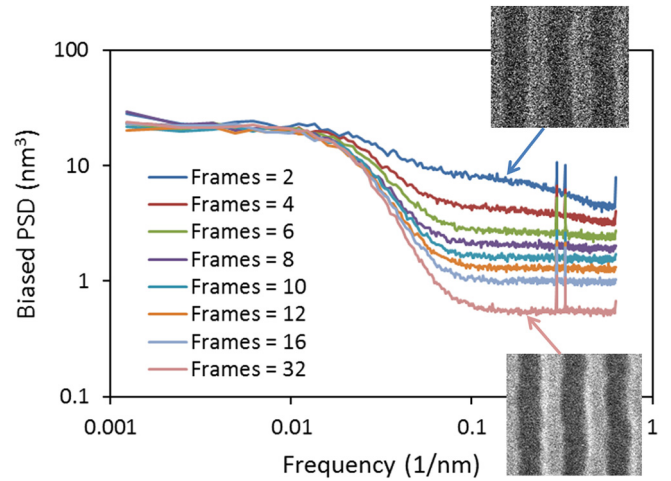


Fig. 3. Power spectral densities (PSDs) of 18 nm resist lines and spaces where only the number of frames of integration was varied. SEM conditions: 500 eV, 49 images per condition, 21 features per image, pixel size = 0.8 nm square, image size = 1024 × 1024 pixels.

Fig. 1 shows that a typical PSD curve can be described with three parameters [7,8]. PSD(0) is the zero-frequency value of the PSD. While this value of the PSD can never be directly measured (zero frequency corresponds to an infinitely long line), PSD(0) can be thought of as the value of the PSD in the flat low-frequency region. The PSD begins to fall near the frequency of $1/(2\pi\xi)$ where ξ is the correlation length. In the fractal region we have “1/f” noise and the PSD has a slope (on the log-log plot) corresponding to a power of $1/f$. The slope is defined as $2H + 1$ where H is called the roughness exponent (or Hurst exponent). The variance of the roughness is the area under the PSD curve and is derived from the other three PSD parameters. The exact relationship between variance and the other three PSD parameters depends on the exact shape of the PSD curve in the mid-frequency region (defined by the correlation length), but an approximate relationship can be used to show the general trend: [9]

$$\sigma^2 \approx \frac{PSD(0)}{(2H + 1)\xi} \quad (1)$$

The most common way to measure feature roughness is the top-down CD-SEM. There are, however, some errors in the SEM images that have large impact on the measured PSD while having almost no impact on the measurement of mean CD. The biggest impediment to accurate roughness measurement is noise in the CD-SEM image. SEM images

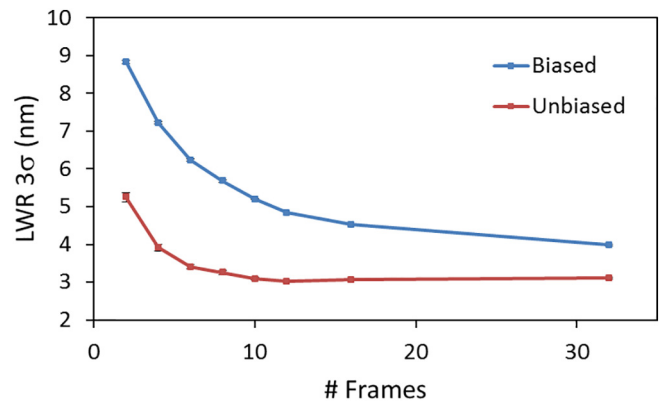


Fig. 4. Biased and unbiased measurements of 3σ linewidth roughness (LWR) as a function of the number of frames of integration. All conditions were the same as described in Fig. 3. Error bars represent 95% confidence interval estimates.

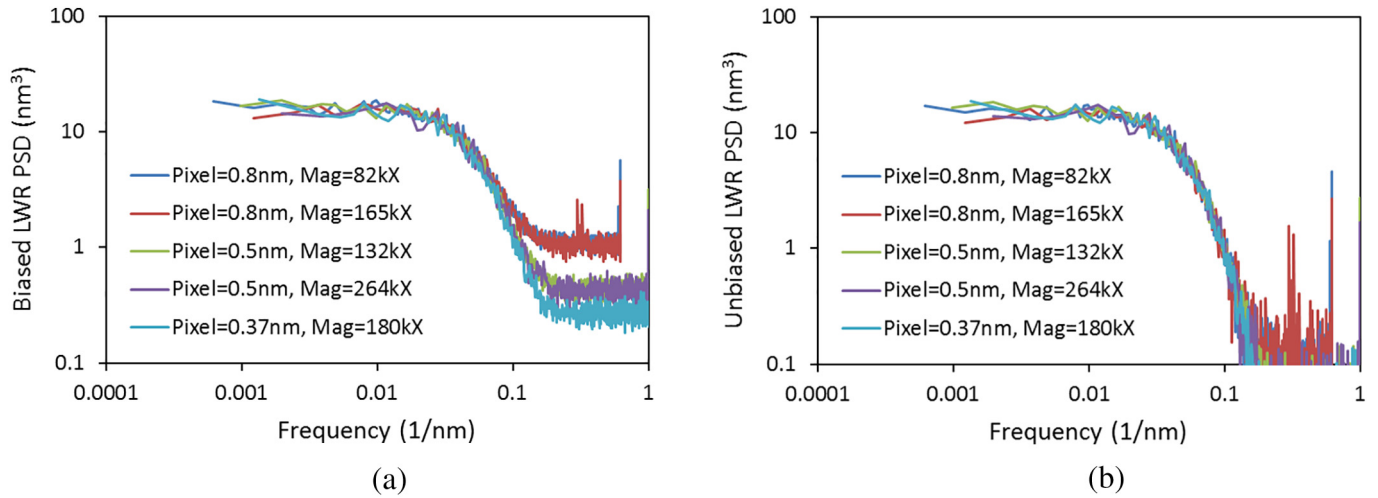


Fig. 5. Power spectral densities as a function of pixel size and magnification showing (a) the biased LWR PSD, and (b) the unbiased LWR PSD after noise has been measured and subtracted off. SEM conditions: 500 eV, 3 images per condition, 16 nm resist lines and spaces.

suffer from shot noise, where the number of electrons detected for a given pixel varies randomly, followed by detector and detector amplification noise. For the expected Poisson distribution, the variance in the number of electrons detected for a given pixel of the image is equal to the mean number of electrons detected. Since the number of detected electrons is proportional to the number of electrons that impinge on that pixel, relative noise can be reduced by increasing the electron dose that the sample is subjected to. For photoresist, however, high electron dose leads to sample damage (resist line slimming).

SEM edge detection noise adds to the actual roughness of the patterns on the wafer to produce a measured roughness that is biased higher [10].

$$\sigma_{biased}^2 = \sigma_{unbiased}^2 + \sigma_{noise}^2 \quad (2)$$

where σ_{biased} is the roughness measured directly from the SEM image, $\sigma_{unbiased}$ is the unbiased roughness (that is, the true roughness of the wafer features), and σ_{noise} is the random error in detected edge position (or linewidth) due to noise in the SEM imaging. Since an unbiased estimate of the feature roughness is obviously what is desired, the measured roughness must be corrected by subtracting an estimate of the noise term.

While several approaches for estimating the SEM noise and subtracting it out have been proposed [1–6], these approaches have not proven successful for today's small feature sizes. The problem is the lack of edge detection robustness in the presence of high image noise: when noise levels are high, edge detection algorithms often fail to find the edge. Image filtering can improve edge detection robustness, but at the expense of irreversibly altering the noise behavior of the image. If edge detection without image filtering can be accomplished, noise measurement and subtraction can be achieved by comparing the PSD behavior of the noise with the PSD behavior of the actual wafer features. We expect resist features (as well as after-etch features) to have a PSD behavior as shown in Fig. 1. Correlations continuously reduce high-frequency roughness so that the roughness becomes very small over

very small length scales. SEM image noise, on the other hand, can be reasonably assumed to be white noise, so that its PSD is flat. Thus, at a high enough frequency, the measured PSD will be dominated by image noise and not actual feature roughness (the so-called “noise floor”). Given the grid size along the length of the line (Δy), SEM noise affects the PSD according to [11]

$$PSD_{w/noise}(f) = PSD_{w/o\ noise}(f) + \sigma_{noise}^2 \Delta y \quad (3)$$

Thus, measurement of the high-frequency PSD (in the absence of any image filtering) provides a measurement of the SEM image noise. Fig. 2 illustrates this approach.

The key to using the above approach of noise subtraction for obtaining an unbiased PSD (and thus unbiased estimates of the parameters $\sigma_{LWR}(\infty)$, $PSD(0)$, and ξ) is to robustly detect edges without the use of image filtering. This can be accomplished using an inverse linescan model [12]. A linescan model predicts the SEM image linescan given a set of beam conditions and the feature geometry on the wafer. Ideally, such a model would be physically based, easily calibrated, and not computationally intensive. An inverse linescan model runs this linescan model in reverse: given a measured linescan, what wafer feature sizes produce a linescan that best fits the data? Such an inverse linescan model can use the physics of SEM image formation to constrain the possible mean linescan shapes and reject the noise in the measured linescan to extract its signal.

Other SEM errors can influence the measurement of roughness PSD as well. For example, SEM field distortion can artificially increase the low-frequency PSD for LER and PPR, though it has little impact on LWR [13]. Background intensity variation in the SEM can also cause an increase in the measured low-frequency PSD, including LWR as well as LER and PPR. If these variations can be measured, they can potentially be subtracted out, producing the best possible unbiased estimate of the PSD and its parameters.

Table 1
Measured PSD parameters for the PSDs shown in Fig. 5.

	Pixel 0.8 nm 82kX	Pixel 0.8 nm 164kX	Pixel 0.5 nm 130kX	Pixel 0.5 nm 264kX	Pixel 0.37 nm 180kX
Biased LWR (3-sigma, nm)	5.10	4.99	4.67	4.61	4.47
Unbiased LWR (3-sigma, nm)	3.66	3.65	3.70	3.67	3.63
Unbiased LWR PSD(0) (nm ³)	15.95	16.18	17.2	16.25	16.35
LWR correlation length (nm)	5.08	5.05	5.31	5.11	5.38

3. Experimental procedure

SEM image acquisition was performed on Hitachi CG-5000 CD-SEM tools. Both extreme ultraviolet (EUV) with a wavelength of 13.5 nm (at 32 nm and 36 nm pitch) and 193 nm immersion (84 nm pitch) lithography processes were investigated. Both after development inspection (ADI) as well as after etch inspection (AEI) images were taken on the CD-SEM.

All analysis of the SEM images was performed with MetroLER (Fractilia, LLC) v1.1 using default settings: the Fractilia Inverse Linescan Model for edge detection, no image filtering, and a threshold setting of 0.5. Power spectral densities used a Welch taper window.

4. Results and discussion

To investigate the influence of SEM imaging parameters, both the magnification and the pixel size were varied. These two parameters can be changed independently by changing the number of pixels in the image (from 512×512 to 2048×2048). Additionally, rectangular shaped pixels were used by setting the magnification to be different in the X and Y directions. Finally, the number of frames of integration was varied from 2 to 32, representing a $16\times$ variation in electron dose.

a. Frames of integration

Total electron dose is directly proportional to the number of frames of integration. Thus, shot noise and its impact on edge detection noise is expected to be proportional to the square root of the number of frames of integration. Fig. 3 shows PSDs of a given resist feature type on a given wafer, measured with different frames of integration. The cases of 6 or more frames of integration exhibit a fairly flat high-frequency noise region. For 2 and 4 frames of integration the noise region is noticeably sloped. Thus, the assumption of white SEM noise is only approximately true, and becomes a more accurate assumption as the number of frames of integration increases.

Fig. 4 shows the biased and unbiased values of the 3σ linewidth roughness measured as a function of the number of frames of integration. The biased roughness varies from 8.83 nm at two frames of integration to 5.68 nm at 8 frames and 3.98 nm at 32 frames. The unbiased roughness, on the other hand, is fairly stable after 6 frames of integration, varying from 5.25 nm at two frames of integration to 3.25 nm at 8 frames and 3.11 nm at 32 frames. While the biased roughness is 43% higher at 8 frames compared to 32, the unbiased roughness is only 4% higher at 8 frames compared to 32. Since the assumption of white SEM noise is not very accurate at 2 and 4 frames of integration, the noise subtraction of the unbiased measurement is not completely successful at these very low frames of integration. Similar results are

Table 2

Relationship between biased and unbiased LWR for a variety of processes. Each of the post-lithography measurements used 16 frames of integration and each of the post-etch measurements used 32 frames.

Process	3σ LWR: biased/unbiased	3σ LWR (nm): biased - unbiased
193i litho, 84 nm pitch, 500 V, 512 rect pixels	1.20	0.76
193i etch, 84 nm pitch, 800 V, 512 rect pixels	1.14	0.43
EUV litho, 32 nm pitch, 500 V, 2048 0.8 nm pixels	1.39	1.44
EUV litho, 32 nm pitch, 500 V, 1024 0.8 nm pixels	1.37	1.34
EUV litho, 32 nm pitch, 500 V, 2048 0.5 nm pixels	1.26	0.97
EUV litho, 32 nm pitch, 500 V, 1024 0.5 nm pixels	1.26	0.94
EUV litho, 32 nm pitch, 500 V, 1024 0.37 nm pixels	1.23	0.84
EUV litho, 36 nm pitch, 500 V, 1024 0.8 nm pixels	1.52	1.86
EUV litho, 32 nm pitch, 500 V, 1024 rect pixels	1.66	2.19
EUV etch, 32 nm pitch, 800 V, 1024 rect pixels	1.09	0.32

obtained for the measurement of LER and PPR. Error bars in the unbiased LWR values in Fig. 4 and subsequent figures are the 95% confidence intervals obtained after adding the variance in biased LWR measurement to the variance in the noise measurement. Biased LWR uncertainty is based on the standard error of the mean of the LWR values for each of the features averaged together. Uncertainty in the noise measurement is based on the standard deviation of the high frequency PSD values about their mean.

b. Pixel size and magnification

Fig. 5 shows the biased and unbiased PSDs for a pattern of 16 nm lines and spaces for different magnifications and pixel sizes. The dose per pixel was kept constant so that the electron shot noise is expected to be independent of pixel size. By Eq. (3), the high frequency values of the PSD will then be smaller for the smaller pixel size (Δy). Table 1 shows the measured 3σ LWR, as well as the other PSD parameters, for these different pixel size and magnification conditions. Under this range of conditions, the biased LWR varied by 0.63 nm (14%), while the unbiased LWR varied by only 0.07 nm (2%). The unbiased LWR is essentially unaffected by these metrology tool settings. Similar results are obtained for the measurement of LER and PPR.

c. Measurement settings with rectangular pixels

In the following, three different measurement processes are compared. Condition A is a 1024×1024 image with a rectangular pixel (0.88 nm in x by 2.5 nm in y) and 8 frames of integration. Condition B is the same as Condition A but with 16 frames of integration. Condition C is a 512×512 image with a rectangular pixel (0.88 nm in x by 5 nm in y) and 16 frames of integration. Three wafers were run through each of these conditions with about 100 images taken per wafer per measurement condition. Fig. 6 plots the resulting unbiased LWR as a function of the biased LWR. As the slope through the data indicates, the unbiased LWR is $5\times$ less sensitive to these measurement conditions compared to the biased LWR. The biggest factor affecting the measured LWR is the number of frames of integration.

d. Biased versus unbiased roughness for a range of processes

The difference between biased and unbiased LWR is not constant, but varies with metrology tool settings, feature size, and process.

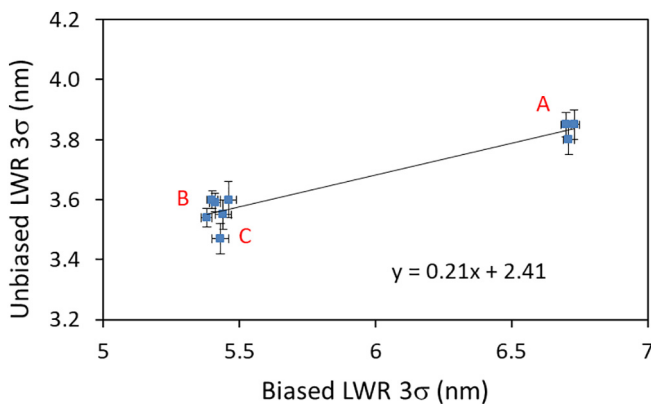


Fig. 6. Comparison of three different SEM measurement recipes on three different wafers. SEM conditions: 500 eV, about 100 images per condition per wafer, 16 nm resist lines and spaces. Results from conditions A, B and C are labeled with those letters.

Likewise the ratio between biased and unbiased LWR varies with metrology tool settings, feature size, and process. Table 2 shows the difference and ratio of biased to unbiased LWR for a variety of conditions. For these conditions, the ratio of biased to unbiased LWR varies from 1.09 to 1.66. The difference between biased and unbiased LWR varies from 0.32 nm to 2.19 nm.

5. Conclusions

A vexing problem with standard roughness measurement today is that the values of the (biased) roughness depend strongly (and in a complicated way) on measurement conditions. It is an important goal of unbiased roughness measurement to reduce as much as possible this sensitivity of measurement results to measurement parameters. In particular, magnification, pixel size, and the number of frames of integration should have only minor effect on the measurement of LWR, LER, and PPR over a usefully wide range of settings.

We have tested a new approach to the unbiased measurement of roughness: the use of an inverse linescan model (as implemented in the MetroLER software). The results show that this unbiased roughness measurement attains the goal of being sufficiently insensitive to measurement settings, providing values that represent the true roughness of the features on the wafers. Varying pixel size and magnification over more than a factor of 2 has essentially no impact on the unbiased LWR, LER, and PPR. The impact of frames of integration on LWR was reduced by more than a factor of 10 as the frames of integration changed by a factor of 4. While other metrology settings and cases should still be tested, this study has proven the usefulness of accurate unbiased roughness measurement.

References

- [1] Benjamin D. Bunday, Michael Bishop, Donald McCormack, et al., Determination of optimal parameters for CD-SEM measurement of line edge roughness, *Metrology, Inspection, and Process Control for Microlithography XVIII*, 5375, SPIE 2004, p. 515.
- [2] J.S. Villarrubia, B.D. Bunday, Unbiased estimation of linewidth roughness, *Metrology, Inspection, and Process Control for Microlithography XIX*, 5752, SPIE 2005, p. 480.
- [3] R. Katz, C.D. Chase, R. Kris, R. Peltinof, J. Villarrubia, B. Bunday, Bias reduction in roughness measurement through SEM noise removal, *Metrology, Inspection, and Process Control for Microlithography XX*, 6152, SPIE 2006, p. 61524L.
- [4] A. Yamaguchi, R. Steffen, H. Kawada, T. Iizumi, Bias-free measurement of LER/LWR with low damage of CD-SEM, *Metrology, Inspection, and Process Control for Microlithography XX*, 6152, SPIE, 2006, 61522D.
- [5] S.-B. Wang, Y.H. Chiu, H.J. Tao, Y.J. Mii, Practical and bias-free LWR measurement by CDSEM, *Metrology, Inspection, and Process Control for Microlithography XXII*, Proc. of SPIE, 6922, 2008, p. 692222.
- [6] Vassilios Constantoudis, Evangelos Gogolides, Noise-free estimation of spatial line edge/width roughness parameters, *Metrology, Inspection, and Process Control for Microlithography XXIII*, 7272, SPIE 2009, pp. 72724B–1.
- [7] Chris A. Mack, Reducing Roughness in Extreme Ultraviolet Lithography, 10450, SPIE, 2017.
- [8] Gian F. Lorusso, Peter Leunissen, Monique Ercken, et al., Spectral analysis of line width roughness and its application to immersion lithography, *J. Micro/Nanolithogr. MEMS MOEMS* 5 (3) (2006) 033003.
- [9] Chris A. Mack, Analytical expression for impact of linewidth roughness on critical dimension uniformity, *J. Micro/Nanolithogr. MEMS MOEMS* 13 (2) (2014) 020501.
- [10] J.S. Villarrubia, B.D. Bunday, Unbiased estimation of linewidth roughness, *Proc. SPIE* 5752 (2005) 480–488.
- [11] Chris A. Mack, Systematic errors in the measurement of power spectral density, *J. Micro/Nanolithogr. MEMS MOEMS* 12 (3) (2013) 033016.
- [12] Chris A. Mack, Benjamin D. Bunday, Using the analytical linescan model for SEM metrology, *Proc. SPIE* 10145, *Metrology, Inspection, and Process Control for Microlithography XXXI*, 2017, 101451R.
- [13] Barton Lane, Chris Mack, Nasim Eibagi, Peter Ventzek, Global minimization line-edge roughness analysis of top down SEM images, *Proc. SPIE* 10145, *Metrology, Inspection, and Process Control for Microlithography XXXI*, 2017, 101450Y.